Identifying a Robust Waste Heat Recovery System for Varying Hot Water Temperature Demand

Maizura Mokhtar
The School of Engineering & the Built Environment
Edinburgh Napier University
Edinburgh EH14 5JH, United Kingdom
m.mokhtar@napier.ac.uk

ABSTRACT

The food and drinks process industry requires large volumes of hot water at varying demand temperatures. To help minimise the cost of energy usage and provide hot water at a required temperature, there has been a growing interest in the installation of a waste heat recovery system coupled to a hot water reservoir (WHRS-HWR). In this paper, we explore how a multi-objective evolutionary algorithm can be used to approximate the Pareto-optimal system configurations of WHRS-HWR installations. In particular, we show how the combined use of clustering and parallel coordinate plots can ease in the trade-off analysis of the resulting configurations, and how it can be used to find a set of robust configurations that work across varying hot water demand temperatures. This demonstrates the role that multi-objective methods with clear visualisation of the results can play in allowing installers to make informed choices in industrial applications.

CCS CONCEPTS

•**Applied computing → Industry and manufacturing; Multi-criterion optimization and decision-making;** *Command and control;*

KEYWORDS

Visualisation; Parallel coordinates; Multi-objective optimisation; Waste heat recovery; Robustness

ACM Reference format:
Maizura Mokhtar. 2017. Identifying a Robust Waste Heat Recovery System for Varying Hot Water Temperature Demand. In *Proceedings of GECCO '17 Companion, Berlin, Germany, July 15-19, 2017,* 8 pages.
DOI: http://dx.doi.org/10.1145/3067695.3082484

1 INTRODUCTION

The installation of a waste heat recovery system coupled to a hot water reservoir (WHRS-HWR) is beneficial for food and drinks process industries, which utilise large refrigeration systems and use large volume of hot water. Waste heat is the heat released from the refrigeration system and that heat can be captured and used to provide hot water from the hot water reservoir (HWR) at a desirable hot water temperature (T_{hw}).

There are many uses for hot water in the food and drinks process industries, and the temperature requirements vary for different uses. For example, high water temperature ($T_{hw} \geq 75$°C) is required for pasteurisation and domestic heating; medium (50°C $\leq T_{hw} \leq$ 75°C) is for cleaning and wash-down; and low temperature ($T_{hw} \leq$ 50°C) is required for domestic use. Given this variability and the high cost of installation for a WHRS-HWR system, it is beneficial to find a system configuration that is robust to the different hot water temperature demand. Such a configuration would enable a company to maintain hot water at varying temperatures, without significantly affecting the efficiency of the system, which could be the case if the coupled WHRS-HWR was initially specified for a hot water temperature that is different to that which is later required.

A multi (and many)-objective evolutionary algorithm (MOEA) is a useful tool that can aid in finding optimal WHRS-HWR system configurations, particularly when the aim is to find a WHRS-HWR configuration that is robust to different parameter settings. MOEAs have been successfully used to optimise many different types of engineering system [1], [3], [7], [14], [13]. An MOEA finds the Pareto-optimal solutions for a given design problem [4]. The set of Pareto-optimal solutions provide choices from which installers can choose from, in order to best suit their needs. However, to enable for an informed choice to be made, the Pareto-optimal solutions and their objectives have to be presented in a way that can be understood by humans. This is often an issue when the number of objectives considered is large ($n > 4$) [5].

Given the variety of hot water demand temperatures in a plant (T_{hw}), it would be useful to understand the correlations between varying desired hot water demand temperature T_{hw} with that of the system configurations, and their impact on the system's efficiencies. If the optimisation is performed on varying T_{hw}, each scenario will have its own Pareto-optimal front and solutions. By analysing the similarities between the fronts, this may provide some information if there is a set of WHRS-HWR configurations that is common for all scenarios. One may then hypothesize that this set of configurations can be considered to be the robust solutions.

To allow for such analysis to occur, visualisation of how the Pareto-optimal solutions correlate to their objectives is important [5], [10]. This paper presents the combined use of clustering and parallel coordinates to display the Pareto-optimal solutions together with their corresponding objective values – as presented in [10]. To ease in the visualisation, Pareto-optimal solutions are first clustered into k-number of clusters in the solution space or in the objective

GECCO '17 Companion, Berlin, Germany

978-1-4503-4939-0/17/07…$15.00
DOI: http://dx.doi.org/10.1145/3067695.3082484

space. This is to identify the degree of commonality between the solutions. The decision as to which space to best perform the clustering in is dependent on the criteria of selection. In the case of the WHRS-HWR, if the requirement is to select the configurations with the least cost and the maximum savings, the clustering is best performed in the objective space. If the size of the system governs the choice, it is better to perform the clustering in the solution space, which will later ease in the visualisation, as there can be solutions that are very dissimilar to each other that are providing similar objective values [10].

For each cluster identified, parallel coordinates [9], [8] are used to visualise the high-dimensional solution space and objective space as a pair of two-dimensional plots. The correlation between a solution and its objective values in a specific cluster are identified by the common colour used in both plots. If k is the number of clusters used, this method of visualisation therefore uses only $2k$ number of figures, easing in the analysis of the trade-offs between the Pareto-optimal solutions [10].

This paper shows how the combination of clustering and parallel coordinate plots are used to find a robust system configuration for a coupled WHRS-HWR from the Pareto-optimal front evolved for varying hot water demand temperature. The paper is divided into five sections: Section 2 describes the coupled WHRS-HWR system and lists the system parameters to be optimised. Three hot water demand temperatures are analysed: low with T_{hw} = 40°C, medium with T_{hw} = 60°C and high with T_{hw} = 78°C. An MOEA is used to find the Pareto-optimal front. Further details with regards to the optimisation are described in Section 3. Section 4 presents the results of the optimisation, and based on the Pareto-optimal fronts obtained and the visualisation method presented, identifies the optimal coupled WHRS-HWR system configuration that is robust to the different hot water temperature demand (T_{hw}). Section 5 concludes the paper.

2 WHRS-HWR

Figure 1 illustrates a typical form of the coupled WHRS-HWR found within the food process industry [11], [10]. The parameters of the coupled WHRS-HWR to be optimised are [11], [10]:

(1) $m_{wt_{max}}$: the maximum mass of water in the HWR, i.e. the capacity of the HWR,
(2) $m_{wt_{min}}$: the minimum mass of water that must be met when the hot water is demanded, also known as the depth of discharge (DoD),
(3) T_{mx}: the maximum temperature level of the HWR,
(4) $P_{b_{max}}$: the maximum power of the back-up heater,
(5) $\dot{m}_{wd_{max}}$: the maximum mass flow rate of the water entering the desuperheater (DSH) of the WHRS.

Identifying the maximum operating level $m_{wt_{max}}$ for the HWR is key to ensuring WHRS-HWR efficiency. The HWR is essentially a battery that stores heat when required. If $m_{wt_{max}}$ is too low when demand takes place, there may be the need to top-up the volume from the main water supply to meet the hot water demand requirement. In a food process industry, hot water is typically required for cleaning and/or pasteurisation when the waste heat availability is low. Because of this, when the top-up is required, the waste heat alone may be insufficient to bring the water temperature (T_{wt}) up to the required operating temperature (T_{hw}). A back-up heater is therefore needed, bringing with it an associated energy cost. It is therefore ideal that $m_{wt_{max}}$ holds a greater volume of water than that which is demanded, with a minimum volume of water that must be maintained when the hot water is demanded from the HWR ($m_{wt_{min}}$). However, $m_{wt_{max}}$ should not be too large, as the cost to install a larger HWR may outweigh the benefits that it may bring.

Setting the $m_{wt_{min}}$ is also key. If $m_{wt_{min}}$ is too high and the water temperature in the HWR is between T_{hw} and T_{mx}, then there will be less opportunity to capture the waste heat, when there is a need to increase the mass of water in the HWR m_{wt} up to $m_{wt_{max}}$ using the main water supply (refill). This is especially the case if $m_{wt_{max}}$ is small.

There will always be a loss of energy to the environment, in this case due to the temperature difference between the contents of the HWR and its surrounding region. To ensure that no external heat is required when hot water is in demand, there is a need to capture an excess of heat in preparation for idle periods, which can be done by keeping the hot water temperature in the HWR (T_{wt}) at a higher temperature: $\Delta T_{max} = T_{mx} - T_{hw} - T_{loss}$. This ensures that T_{hw} is met, despite the loss of heat to the environment (T_{loss}). However, if T_{mx} is too high, unanticipated demand requires cold water to be injected in order to reach T_{hw}.

In order to evaluate the impact of different design choices, a simulation model was constructed using Simulink®. The model uses thermodynamics equations to simulate the temperature changes in the HWR given the discharge temperature of the refrigerant [12], the demand of the hot water, and the energy lost to the environment. A synthetic data set was created to model the demands for refrigeration (the waste heat source) and hot water (the waste heat sink) within this system. The data is indicated in Figure 2, and is based on the patterns observed within two different dairy processing sites in Scotland. The mass flow rate of the demanded hot water is at 0.556 kg/s, when in demand. More details on this are described in [10].

2.1 Control options

To adapt to operating conditions, it is often desirable to manipulate the settings of system parameters during operation. It is then useful to investigate the correlation between the granularity of the resulting control system and the physical system configuration of the WHRS-HWR, and how the combination of the two impact on the system's efficiency. Because of this, two methods of controls were incorporated into the analysis. The first method is based on a simple binary switch that controls the power output of the back-up heater: $P_b = P_{b_{max}}$ when $T_{wt} < T_{hw}$ and $P_b = 0$, otherwise; and the mass flow rate of water into the WHRS, $\dot{m}_{wd}$: $\dot{m}_{wd} = \dot{m}_{wd_{max}}$. $\dot{m}_{wd}$ is from the main water supply when $m_{wt} < m_{wt_{max}}$ and $\dot{m}_{wd}$ is from the HWR, otherwise. This is the most common method of controls for existing installations.

The second proposed method provides higher granularity of controls, assuming that the amount of fuel for the back-up heater and $\dot{m}_{wd}$ can be varied accordingly, with the use of variable speed pump or solenoid valve. P_b is varied according to the water temperature in the HWR, T_{wt} (1)–(3). When m_{wt} has reached $m_{wt_{max}}$,

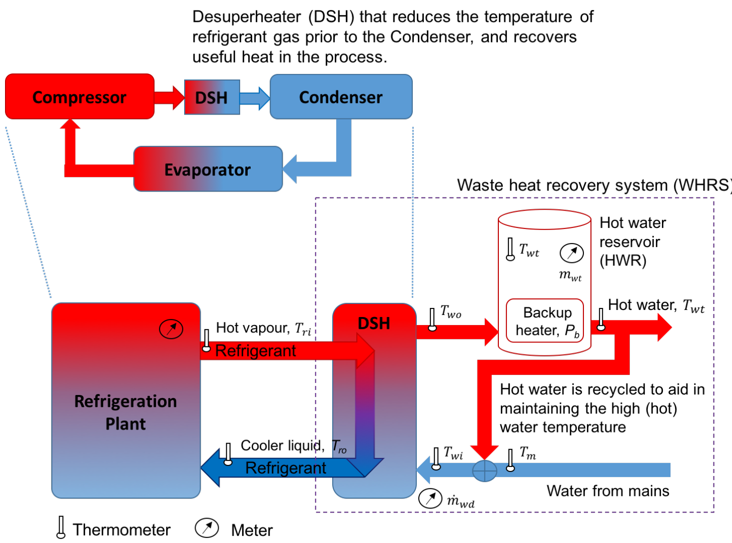

Figure 1: A WHRS comprising of a desuperheater (DSH) and a HWR [10]. Waste heat is provided by the refrigeration plant.

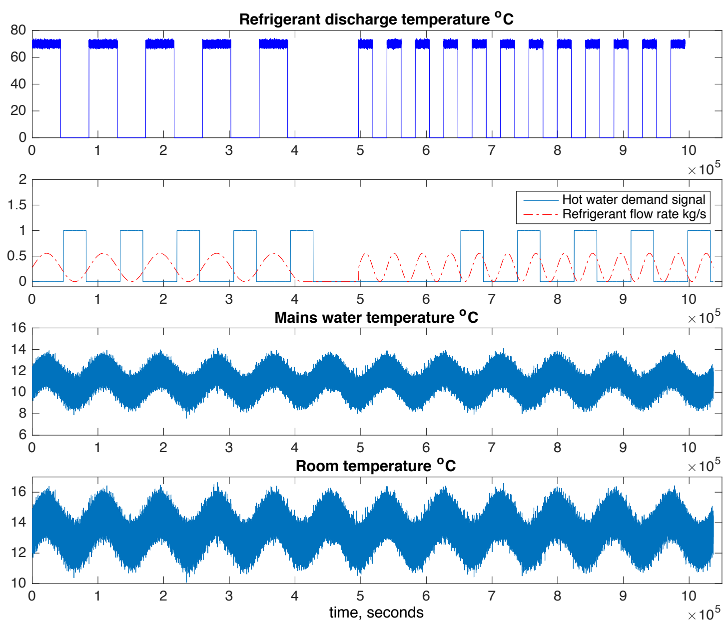

Figure 2: The properties of the refrigerant, hot water demand and the environmental conditions affecting the WHRS.

the water into the WHRS is from the HWR and $\dot{m}_{wd}$ will be varied according to the temperature gradient between the input refrigerant T_{ri} and the intake water T_{wi} (4)–(6), with $T_{wi} = T_{wt}$. When $m_{wt} < m_{wt_{max}}$, the intake water is from main water supply with $\dot{m}_{wd} = \dot{m}_{wd_{max}}$ and T_{wi} is the mains water temperature indicated in Figure 2.

$$P_b = r_p \times P_{b_{max}} \tag{1}$$

$$r_p = \begin{cases} 1 & \text{if } r_{t_p} > 0.75 \\ 0.75 & \text{else if } 0.5 < r_{t_p} \leq 0.75 \\ 0.5 & \text{else if } 0.25 < r_{t_p} \leq 0.5 \\ 0.25 & \text{else if } 0 < r_{t_p} \leq 0.25 \\ 0 & \text{otherwise} \end{cases} \tag{2}$$

$$r_{t_p} = \frac{(T_{hw} - T_{wt})}{T_{hw} \times 0.5} \tag{3}$$

$$\dot{m}_{wd} = r_{wd} \times \dot{m}_{wd_{max}} \tag{4}$$

$$r_{wd} = \begin{cases} 1 & \text{if } r_{t_w} > 0.75 \\ 0.75 & \text{else if } 0.5 < r_{t_w} \leq 0.75 \\ 0.5 & \text{else if } 0.25 < r_{t_w} \leq 0.5 \\ 0.25 & \text{otherwise} \end{cases} \tag{5}$$

$$r_{t_w} = \frac{(T_{ri} - T_{wi})}{T_{wi} \times 0.25} \tag{6}$$

3 OPTIMISATION OF THE WHRS-HWR

Optimisation was performed for the three hot water demand temperatures, with each evaluated using the two control methods described in Section 2.1. NSGA-II was used for optimisation[1], and this was implemented in Matlab® using the typical NSGA-II variation operators indicated in [6]: mutation probability = 1/number of evolved parameters, distribution index for crossover = 20, distribution index for mutation = 100, population size = 200, no. of generations = 100. Table 1 lists the limits for the evolved parameters. The limits were added to bound the search space and to speed up the convergence of the algorithm. m_{wt} and T_{wt} are initialised with the evolved $m_{wt_{max}}$ at T_{hw}. NSGA-II was chosen because reviews conducted by [2] indicated that NGSA-II outperformed other MOEAs, including ESPEA and NSGA-III when optimising a smart building's energy storage system, a system with notable similarities to a WHRS [11].

The objectives that govern the optimisation are [11], [10]:

(1) to minimise the need for back-up energy when the heat captured by the WHRS is insufficient to meet demand,
(2) to maximise the overall savings when using the WHRS, i.e. the difference in the external energy usage with and without the WHRS installation,
(3) to minimise the temperature difference when the demanded temperature was not met,
(4) to minimise the temperature difference when the HWR water temperature exceeds the demand,
(5) to minimise the exceeding mass of water in the HWR from its maximum limit of $m_{wt_{max}}$, when the water is replenished from the main,
(6) to minimise the waste heat not captured.

Objectives 1, 3, 4 and 5 are motivated by the desire to reduce the overall cost of energy and water usage. Objectives 2, 4 and 6 reduce overall energy wastage, which in turn reduces CO_2 emissions. These objectives promote mutually conflicting design choices, therefore the use of an MOEA is ideal. Objective 1, for instance, can be minimised by using a small reservoir; objectives 2 and 6, by comparison, will potentially be optimised when a large HWR is used. Objectives 5 and 6 benefit from a small $\dot{m}_{wd_{max}}$ and $P_{b_{max}}$; objective 3 benefits with small $\dot{m}_{wd_{max}}$ and large $P_{b_{max}}$; and objective 4 benefits with large $\dot{m}_{wd_{max}}$ but small $P_{b_{max}}$ [10].

[1] Although any MOEA can be used to optimise the system, as long as a Pareto-optimal front is obtained, for which the analysis to find the set of robust solutions for varying requirements can be made.

Table 1: Limits for the evolved parameters.

Parameter	Min	Max
$m_{wt_{max}}$	1.0×10^3 kg	50.0×10^3 kg
$m_{wt_{min}}$ (%age of $m_{wt_{max}}$)	10 %	100 %
ΔT_{max} (°C)	0°C	98°C − T_{hw}
$P_{b_{max}}$ (kW)	100kW	1000kW
$\dot{m}_{wd_{max}}$ (kg/s)	0.5 kg/s	1.0 kg/s

4 RESULTS: IDENTIFYING A ROBUST SOLUTION

Given that the coupled WHRS-HWR consists of large and/or heavy equipments that will be difficult to install and disassemble, a robust physical system configuration which is Pareto-optimal across all objectives and is common for a number of scenarios is best identified prior to its installation. By analysing the Pareto-optimal fronts from various scenarios, i.e. varying T_{hw} and different controller configurations, a set of common system configurations can be identified. This set of common configurations are the solutions that can be considered as the robust solutions, and are therefore good choices for installation.

The Pareto-optimal solutions can be visualised using parallel coordinates. To enable the plots to share a common y-axes, the solutions and the objective values are normalised. The solutions are normalised using the minimum and maximum values listed in Table 1. The minimum and maximum values used to normalise the objective values are indicated in Table 2.

The number of clusters used will depend on the information that is required from the solutions. Given that the objective is to find the set of solutions robust to varying scenarios, clustering is performed in the solution space using the k-means clustering algorithm. The number of clusters used is governed by the distribution of the solutions and the ability to extract useful information from the figures. More details on this are presented in [10].

Six objectives were used for optimisation. However, the main objective that drives the decision for a company is typically the need to achieve maximum savings at a minimum cost. The other objectives ensure the efficient use of the WHRS-HWR. By analysing the parallel coordinate plots in Figures 3–5, where for each cluster the correlation between a solution to its objective values is identified by its common colour, the system attributes common across the three design scenarios that will achieve these criteria are:

(1) Large HWR tank size, capable of occupying $m_{wt_{max}} \geq 1.5 \times$ the mass of water required in a day. Based on Figure 2, approximately 24×10^3 kg of water is required per day.
(2) Low $m_{wt_{min}}$, whereby $m_{wt_{min}} \leq (0.5 m_{wt_{max}})$, when the hot water is in demand. The value for $m_{wt_{min}}$ depends on the $m_{wt_{max}}$, the T_{hw} and the amount of water required.
(3) Low $P_{b_{max}}$, with $P_{b_{max}}$ no higher than 600kW.
(4) Small $\dot{m}_{wd_{max}}$, with $\dot{m}_{wd_{max}}$ no greater than 0.6 kg/s,

Any of the evolved system parameters' normalised value ≥ 0.5 is considered as large or high, and small or low otherwise. These system attributes correspond to the solutions in the following clusters:

(1) For T_{hw} = 40°C: clusters 3 and 7 in Figure 3a, and cluster 7 in Figure 3b

Table 2: The max and min values used for normalisation of the objectives' values in the Figures 3 – 5.

Objectives	78°C		60°C		40°C	
	Max	Min	Max	Min	Max	Min
1. To minimise back-up energy	14.618 MWh	7.852 MWh	10.356 MWh	6.5256 MWh	5.7793 MWh	2.5120 MWh
2. To maximise the savings	17.27 %	0.44 %	27.20 %	6.21 %	57.01 %	13.39 %
3. To minimise the temperature difference with the demand temperature was not met	34.4819 °C	0 °C	22.4781 °C	0 °C	5.8854 °C	0 °C
4. To minimise the temperature difference with the demand temperature has been exceeded	20.3938 °C	0 °C	31.8732 °C	0 °C	44.2305 °C	0 °C
5. To minimise the exceeding mass of water in the HWR	59.6098 kg	8.3827 kg	58.4071 kg	16.6283 kg	56.7865 kg	2.6323 kg
6. To minimise the waste heat not captured	39.48 %	0 %	38.98 %	0 %	41.66 %	0 %

(2) For T_{hw} = 60°C: cluster 8 in Figure 4a, and cluster 1 in Figure 4b
(3) For T_{hw} = 78°C: cluster 4 in Figure 5b.

The HWR with T_{hw} = 40°C will require a lower maximum rated $P_{b_{max}}$ for the back up heater, in comparison to when a higher T_{hw} is required. Lower $P_{b_{max}}$ is sufficient because of the smaller temperature gradient between T_{hw} and the water temperature from the main water supply. Solutions for T_{hw} = 40°C will also require a lower ΔT_{max}. Given that the temperature gradient between T_{hw} and the ambient temperature is lower for T_{hw} = 40°C, in comparison to the others, the rate of heat loss will also be lower, and therefore the amount of heat needed to accommodate for the heat loss will also be lower.

5 CONCLUSION

This paper describes the use of an MOEA to approximate the Pareto-optimal configurations for a waste heat recovery system (WHRS) coupled to a hot water reservoir (HWR). To ensure clear visualisation of results and to find the configurations that are robust to varying hot water demand temperature (T_{hw}), the Pareto front is first clustered to find common attributes, prior to the visualisation of the configurations and their objectives. Parallel coordinates are used to visualise the clustered solutions. The results show that if a company requires a design solution that is robust, the ideal system configuration will be that which has a large maximum size of the HWR, with low rated power of the backup heater and small maximum flow rate of the water flowing into the WHRS-HWR. More generally, the results demonstrate how the combined use of clustering and parallel coordinates can usefully contribute to the analysis of Pareto-optimal sets.

The results also show that the coupled WHRS-HWR can benefit from the use of a controller which provides higher granularity controls. One such example of a controller is the rule-based system indicated in this paper. Others include, but are not limited to, PID or Artificial Neural Networks; although for these controllers, it would be ideal for the controller's parameters to be evolved together with the system's configuration to ensure efficiency. It seems likely that the presented visualisation approach would help in the analysis of how the control system parameters correlate with the WHRS-HWR system configuration.

6 ACKNOWLEDGMENT

The work is funded by Innovate UK (101995), EPSRC (EP/M507180/1) and Edinburgh Napier University (Research Funding Competition).

REFERENCES

[1] A. Arias-Montano, C. A. C. Coello, and E. Mezura-Montes. 2012. Multiobjective Evolutionary Algorithms in Aeronautical and Aerospace Engineering. *IEEE Transactions on Evolutionary Computation* 16, 5 (Oct 2012), 662–694.

[2] Marlon Braun, Thomas Dengiz, Ingo Mauser, and Hartmut Schmeck. 2016. Comparison of Multi-objective Evolutionary Optimization in Smart Building Scenarios. In *Applications of Evolutionary Computation: 19th European Conference, EvoApplications 2016, Porto, Portugal, March 30 - April 1, 2016, Proceedings.* Springer International Publishing.

[3] Salvatore Carlucci, Giulio Cattarin, Francesco Causone, and Lorenzo Pagliano. 2015. Multi-objective optimization of a nearly zero-energy building based on thermal and visual discomfort minimization using a non-dominated sorting genetic algorithm (NSGA-II). *Energy and Buildings* 104 (2015), 378 – 394.

[4] Carlos A Coello Coello and Gary B Lamont. 2004. *Applications of multi-objective evolutionary algorithms.* Vol. 1. World Scientific.

[5] K. Deb and H. Jain. 2012. Handling many-objective problems using an improved NSGA-II procedure. In *2012 IEEE Congress on Evolutionary Computation.* 1–8.

[6] K. Deb, A. Pratap, S. Agarwal, and T. Meyarivan. 2002. A fast and elitist multiobjective genetic algorithm: NSGA-II. *Evolutionary Computation, IEEE Transactions on* 6, 2 (Apr 2002), 182–197.

[7] Bhargav Gadhvi, Vimal Savsani, and Vivek Patel. 2016. Multi-Objective Optimization of Vehicle Passive Suspension System Using NSGA-II, {SPEA2} and PESA-II. *Procedia Technology* 23 (2016), 361 – 368. 3rd International Conference on Innovations in Automation and Mechatronics Engineering 2016, {ICIAME} 2016 05-06 February, 2016.

[8] A. Inselberg. 1997. Multidimensional detective. In *Information Visualization, 1997. Proceedings., IEEE Symposium on.* 100–107.

[9] Alfred Inselberg. 2009. *Parallel Coordinates: Visual Multidimensional Geometry and Its Applications.* Springer-Verlag New York, Inc., Secaucus, NJ, USA.

[10] Maizura Mokhtar, Stephen Burns, Dave Ross, and Ian Hunt. 2017. Exploring multi-objective trade-offs in the design space of a waste heat recovery system. *Applied Energy* 195 (2017), 114 – 124.

[11] Maizura Mokhtar, Ian Hunt, Stephen Burns, and Dave Ross. 2016. Optimising a Waste Heat Recovery System Using Multi-Objective Evolutionary Algorithm. In *Proceedings of the 2016 on Genetic and Evolutionary Computation Conference Companion (GECCO '16 Companion).* ACM, New York, NY, USA, 913–920.

[12] Douglas T Reindl and Todd B Jekel. 2007. Heat recovery in industrial refrigeration. *ASHRAE Journal* 49, 8 (2007), 22–29.

[13] Victor Tulus, Dieter Boer, Luisa F. Cabeza, Laureano Jiménez, and Gonzalo Guillén-Gosálbez. 2016. Enhanced thermal energy supply via central solar heating plants with seasonal storage: A multi-objective optimization approach. *Applied Energy* 181 (2016), 549 – 561.

[14] Chuan Zhang, Li Zhou, Pulkit Chhabra, Sushant S. Garud, Kevin Aditya, Alessandro Romagnoli, Gabriele Comodi, Fabio Dal Magro, Antonella Meneghetti, and Markus Kraft. 2016. A novel methodology for the design of waste heat recovery network in eco-industrial park using techno-economic analysis and multi-objective optimization. *Applied Energy* 184 (2016), 88 – 102.

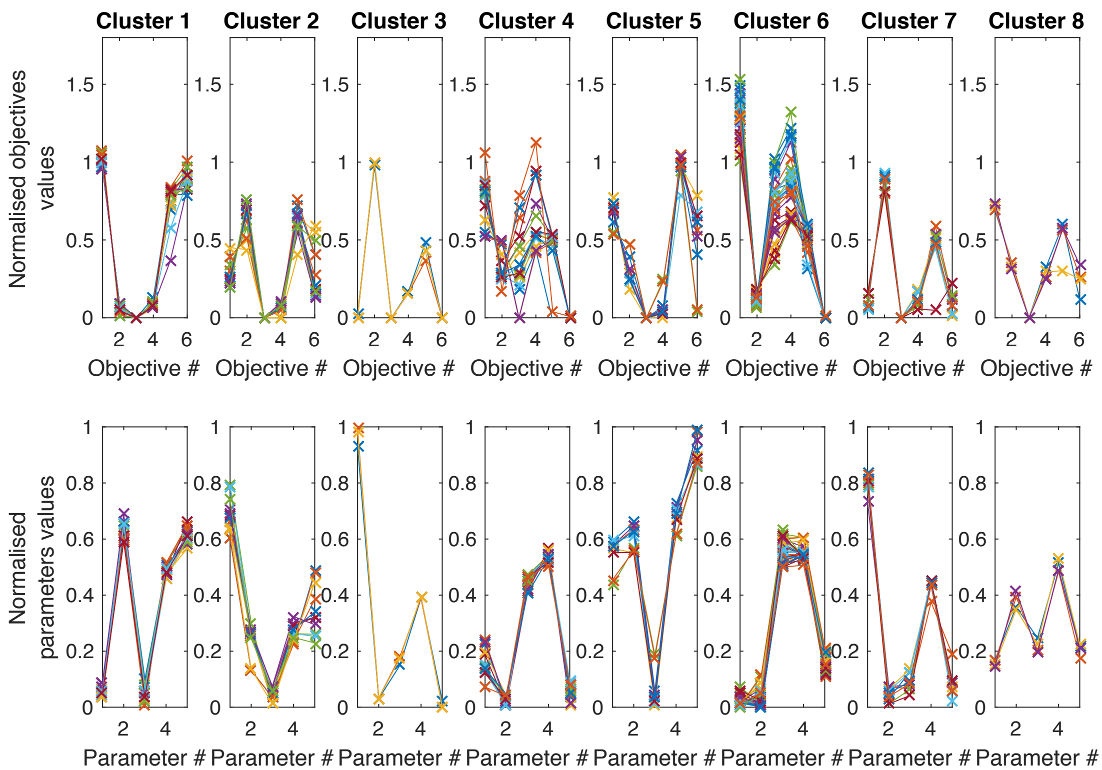

(a) On-Off controller

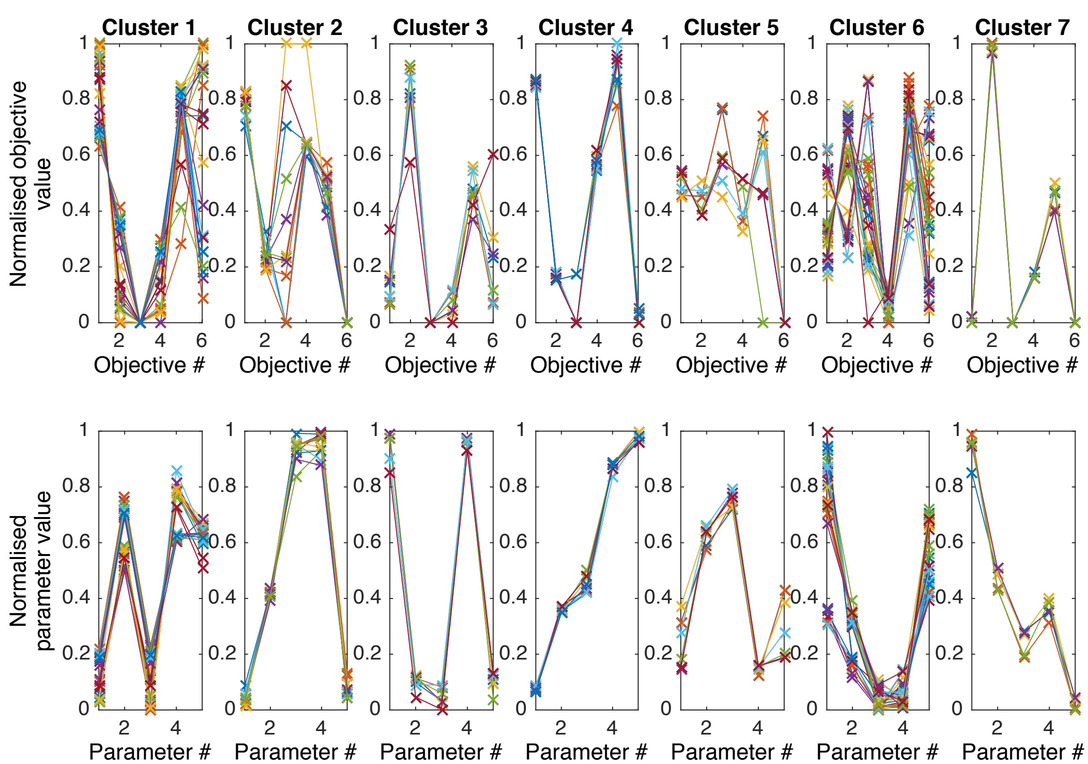

(b) Rule-based controller

Figure 3: Parallel coordinate plots showing clusters of solutions in the Pareto set when clustering is carried out in solution space. The figures are for $T_{hw} = 40$°C.

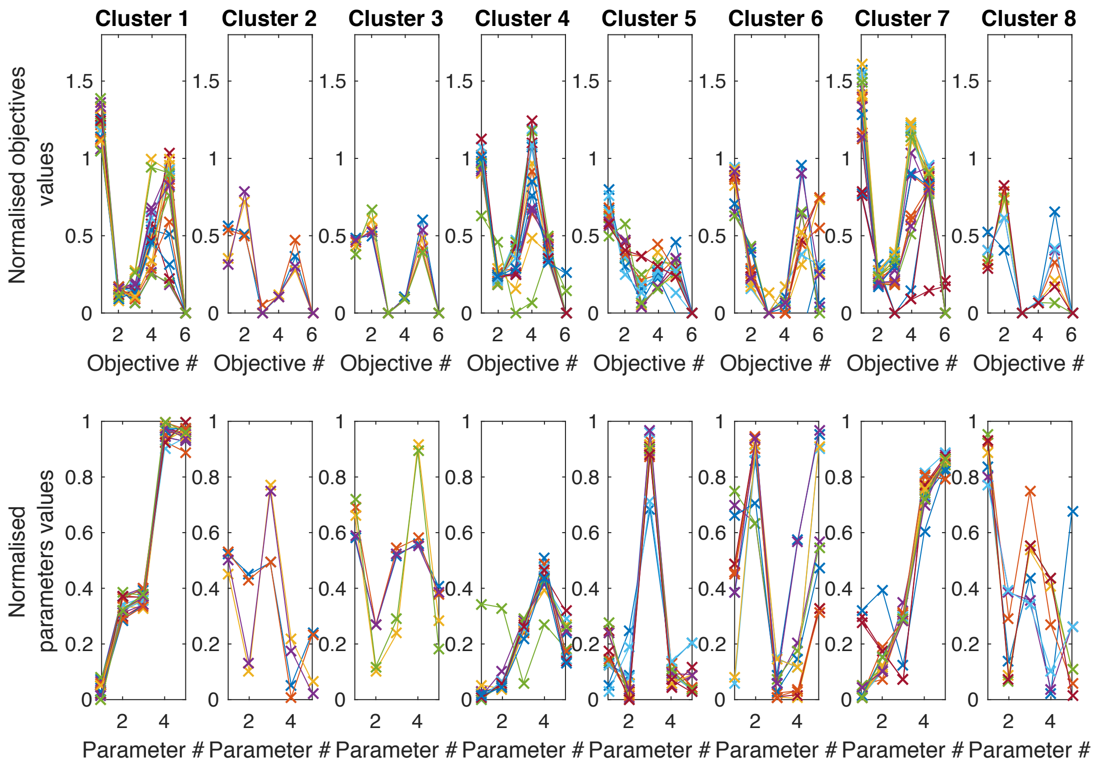

(a) On-Off controller

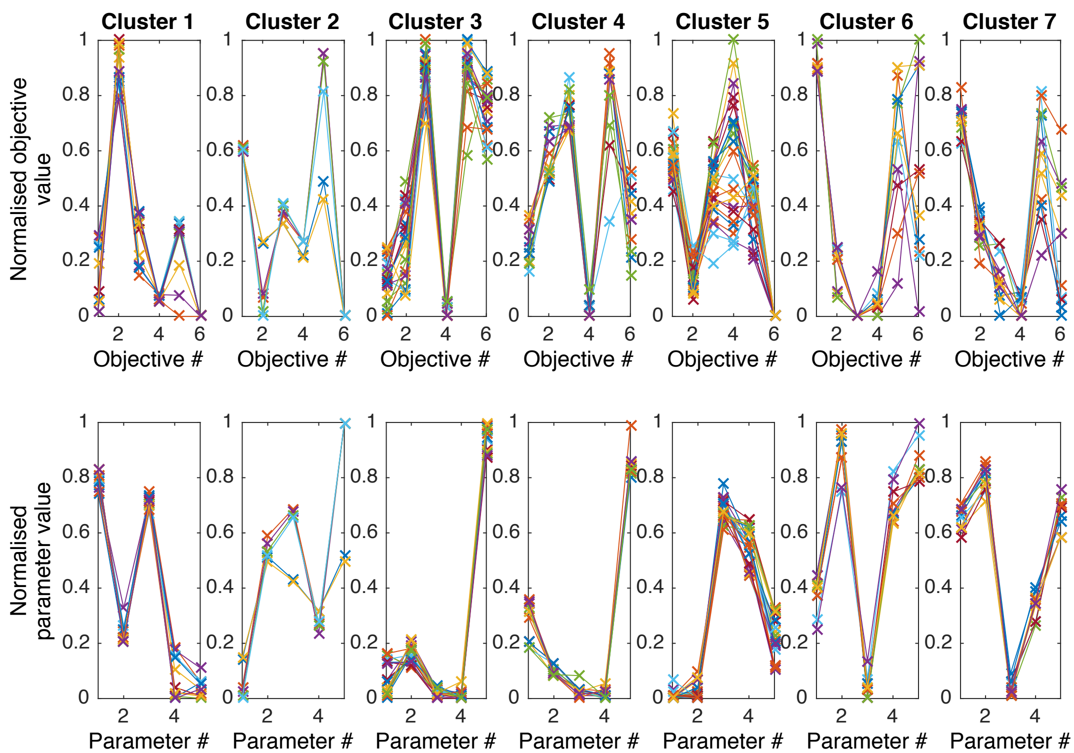

(b) Rule-based controller

Figure 4: Parallel coordinate plots showing clusters of solutions in the Pareto set when clustering is carried out in solution space. The figures are for $T_{hw} = 60$°C.

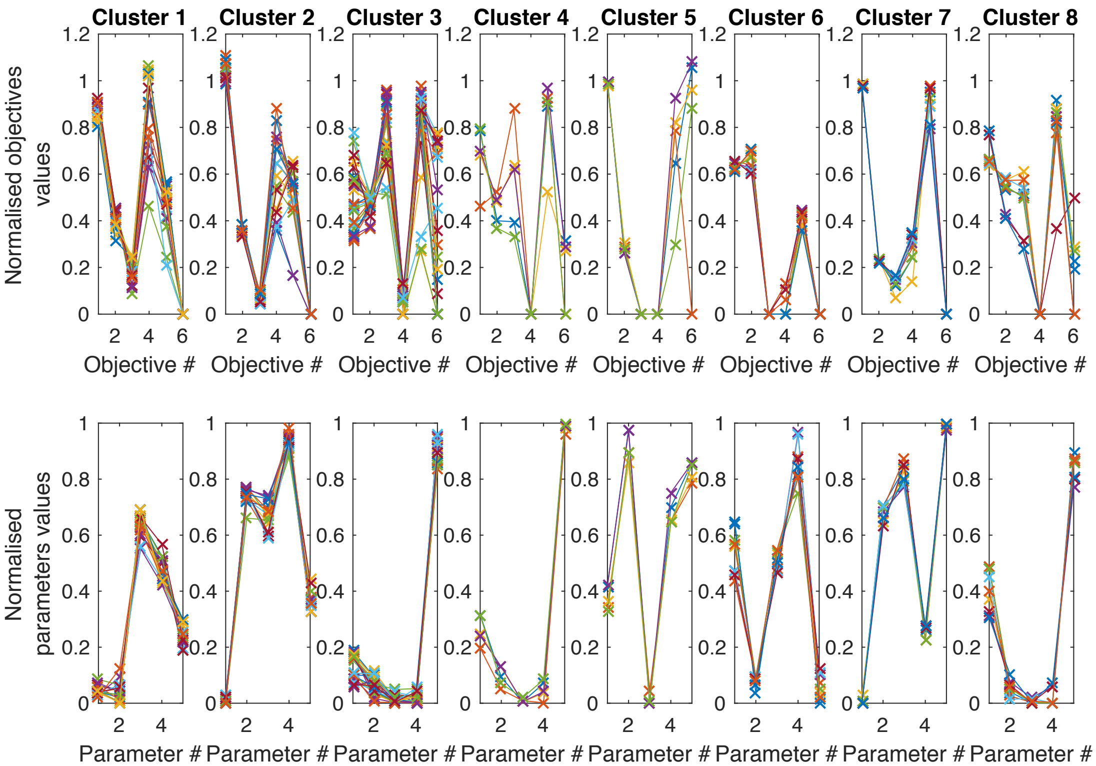

(a) On-Off controller

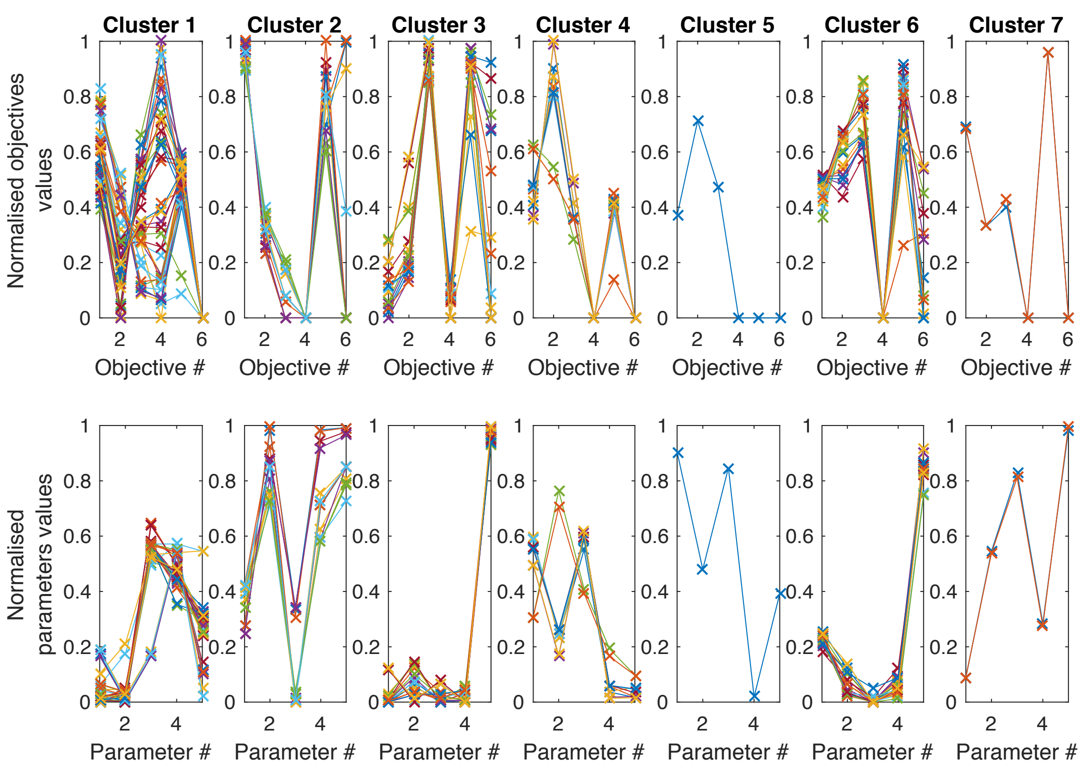

(b) Rule-based controller

Figure 5: Parallel coordinate plots showing clusters of solutions in the Pareto set when clustering is carried out in solution space. The figures are for T_{hw} = 78°C.